



Oscillatory subcooled flow boiling heat transfer of R-134a and associated bubble characteristics in a narrow annular duct due to flow rate oscillation



S.L. Wang, C.A. Chen, T.F. Lin*

Department of Mechanical Engineering, National Chiao Tung University, 1001 University Road, Hsinchu City 30010, Taiwan

ARTICLE INFO

Article history:

Received 26 August 2012
Received in revised form 2 April 2013
Accepted 7 April 2013
Available online 30 April 2013

Keywords:

Oscillatory subcooled flow boiling
R-134a boiling heat transfer
Bubble characteristics
Flow rate oscillation

ABSTRACT

An experiment is conducted here to investigate how an imposed time periodic flow rate oscillation in the form of a triangular wave affects the long time subcooled flow boiling heat transfer and associated bubble characteristics of refrigerant R-134a in a horizontal narrow annular duct. In the experiment the mean R-134a mass flux \bar{G} varies from 200 to 500 kg/m² s, imposed heat flux ranges from 0 to 45 kW/m², and the amplitude of the mass flux oscillation changes from 0 to 30% of \bar{G} with the period of the mass flux oscillation varied from 20 to 120 s for the inlet liquid subcooling ranging from 0 to 6 °C. The duct gap is fixed at 2.0 mm. The results indicate that the inlet liquid subcooling significantly affects the oscillatory flow boiling heat transfer characteristics. Besides, when the imposed heat flux is close to that for the onset of stable flow boiling, intermittent flow boiling appears. The intermittent boiling prevails in a very different range of the Boiling number for a change in the inlet subcooling. Moreover, in the subcooled boiling the heated wall temperature, bubble departure diameter and frequency, and active nucleation site density also oscillate periodically in time. Furthermore, in the persistent boiling at high imposed heat flux the resulting T_w oscillation is stronger for a higher inlet liquid subcooling and for a longer period and a larger amplitude of the mass flux oscillation. And for a larger amplitude of the mass flux oscillation, stronger temporal oscillations in d_p , f and n_{ac} are noted. Finally, a flow regime map is provided to delineate the boundaries separating different boiling regimes for the oscillatory R-134a subcooled flow boiling in the annular duct.

© 2013 Elsevier Ltd. All rights reserved.

1. Introduction

Energy efficiency improvement in various engineering systems is receiving ever increasing attention worldwide intending to reduce the release of CO₂(g) to the atmosphere during the combustion of fossil fuels. Recently, the use of variable frequency, instead of ON/OFF, compressors in air conditioning and refrigeration systems to meet the temporally changing thermal load has been found to significantly augment their energy efficiencies. In these systems the refrigerant flow rate varies with time to accommodate the changing thermal load. How the time varying refrigerant flow rate and heat flux affect the characteristics of boiling and condensation processes in the refrigeration cycles employed in these systems remains largely unexplored.

Flow boiling of refrigerants at constant flow rate in small ducts subject to time independent heating has received some attention. Boiling heat transfer of various fluids in a small duct can be dominated by nucleation or convection depending on the levels of im-

posed heat flux, wall superheats and vapor quality [1–5]. Besides, at lower liquid subcooling bubble nucleation was found to be more important [6]. Moreover, boiling heat transfer is better for smaller duct and liquid subcooling and bubbles in the flow are suppressed to become smaller by raising the flow rate and subcooling [7].

For several decades, different forms of dynamic instabilities in the flow boiling of various liquids in a long heated channel have been recognized [8]. Significant temporal oscillations in pressure, temperature, mass flux and boiling onset occur at certain operating conditions. In a study for R-11 in a long horizontal tube, Ding et al. [9] examined the dependence of the oscillation amplitude and period on the system parameters and located the boundaries among various types of the oscillations. A similar experimental study was carried out by Comakli et al. [10] and the effect of the channel length on the boiling flow dynamic instabilities was examined.

The dynamic behavior of boiling flow in a horizontal channel connected with a surge tank for liquid supply has received some attention [11]. The boiling onset in an upward flow of subcooled water in a vertical tube of 7.8-m long could cause substantial flow pressure and density-wave oscillations [12]. These boiling-onset oscillations were attributed to a sudden increase of pressure-drop

* Corresponding author.

E-mail address: tflin@mail.nctu.edu.tw (T.F. Lin).

Nomenclature

A_s	outside surface area of the heated inner pipe (m^2)	Q_r	net power input (W)
A_{Tw}	amplitude of the heated wall temperature oscillation ($^{\circ}\text{C}$)	t	time instant (sec)
\overline{Bo}	Boiling number, $\overline{Bo} = \frac{q}{G_r i_{fg}}$ (dimensionless)	t_c	time constant (sec)
D_i, D_o	inner and outer diameters of duct (m)	t_o	time instant at beginning of a periodic cycle (sec)
D_h	hydraulic diameter, $D_h = (D_o - D_i)$, (m)	t_p	period of mass flux oscillation (sec)
d_p	bubble departure diameter (mm)	$\Delta T_{sat}, \bar{T}_{sat}$	instantaneous and time-average saturated temperature of refrigerant ($^{\circ}\text{C}$)
f	bubble departure frequency (1/s)	T_w	temperature of heated wall ($^{\circ}\text{C}$)
G, \bar{G}	instantaneous and time-average mass fluxes ($\text{kg}/\text{m}^2 \text{ s}$)	z	coordinate (downstream coordinate for annular duct flow) (mm)
h_r	boiling heat transfer coefficient ($\text{W}/\text{m}^2 \text{ }^{\circ}\text{C}$)		
i_{fg}	enthalpy of vaporization (J/kg)	<i>Greek symbols</i>	
n_{ac}	active nucleation site density (n/m^2)	ΔG	amplitude of mass flux oscillation ($\text{kg}/\text{m}^2 \text{ s}$)
\bar{P}, P_m	mean system pressure and instantaneous inlet pressure (kPa)	ΔT_{sat}	wall superheat, ($T_w - T_{sat}$) ($^{\circ}\text{C}$)
q	imposed heat flux (W/m^2)	$\Delta \bar{T}_{sub}$	time-average inlet liquid subcooling ($^{\circ}\text{C}$)
q_b	heat flux due to bubble nucleation (latent heat transfer) (W/m^2)	δ	duct gap (mm)
q_{ONB}, \bar{q}_{ONB}	steady-state and time-average heat flux for the onset of nucleate boiling (W/m^2)		

across the channel and a large fluctuation in the water flow rate at the onset of nucleate boiling. The effects of the inlet flow conditions on the boiling instabilities were found to be relatively significant [13]. A similar study for subcooled flow boiling of deionized water was conducted by Shuai et al. [14] and the pressure-drop

oscillation was also noted. Reviews of two-phase flow dynamic instabilities in tube boiling have been conducted recently by Kakac and Bon [15] and Tadrist [16].

In view of its importance on thermal hydraulic safety of nuclear reactors, how an inlet flow oscillation affects the critical heat flux

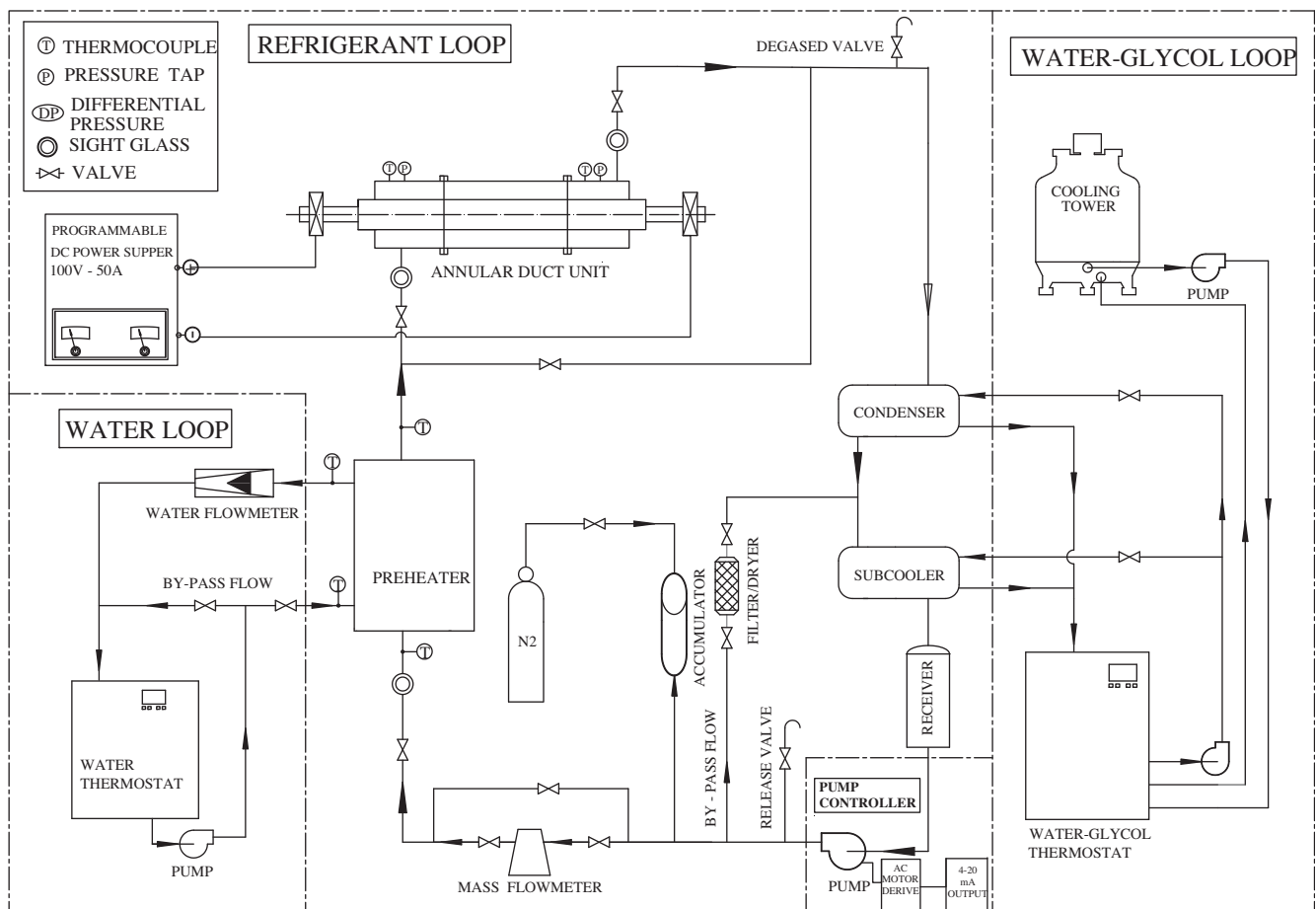


Fig. 1. Schematic of experimental system for flow boiling in annular duct.

of water in boiling channels has been intensively investigated at low mass flux and pressure conditions [17–24]. Significant reduction in the critical heat flux by the flow oscillation was noted. However, to the knowledge of the authors the effects of an inlet flow oscillation on the nucleate boiling heat transfer have not been reported in the open literature.

Considerable amount of works was carried out in the past to examine bubble characteristics associated with stable subcooled flow boiling of various liquids in a duct. It was noted that the bubble departure frequency was suppressed by raising the mass flux and subcooling of R-134a, and only the liquid subcooling significantly affected the bubble size [25]. But the bubble departure frequency increases with the heat flux and the bubble growth rate dropped sharply after the bubble lift-off [26]. Besides, the waiting

time between two bubble cycles decreases significantly at increasing mass flux [27]. Moreover, the size of coalesced bubbles decreases for an increase in the water mass flux and the mass flux only exhibits a strong effect on the bubble size [28].

The above literature review clearly indicates that the unsteady flow boiling heat transfer of HFC refrigerants in small diameter channels resulting from time varying mass flux and/or heat flux remains largely unexplored. In a recent study [29], we experimentally investigated the time periodic saturated flow boiling heat transfer and associated bubble characteristics for R-134a in a horizontal narrow annular duct due to flow rate oscillation. In the present study we move further to investigate how the liquid subcooling affects the R-134a flow boiling in the same duct subject to the same periodic flow rate oscillation. The effects of the ampli-

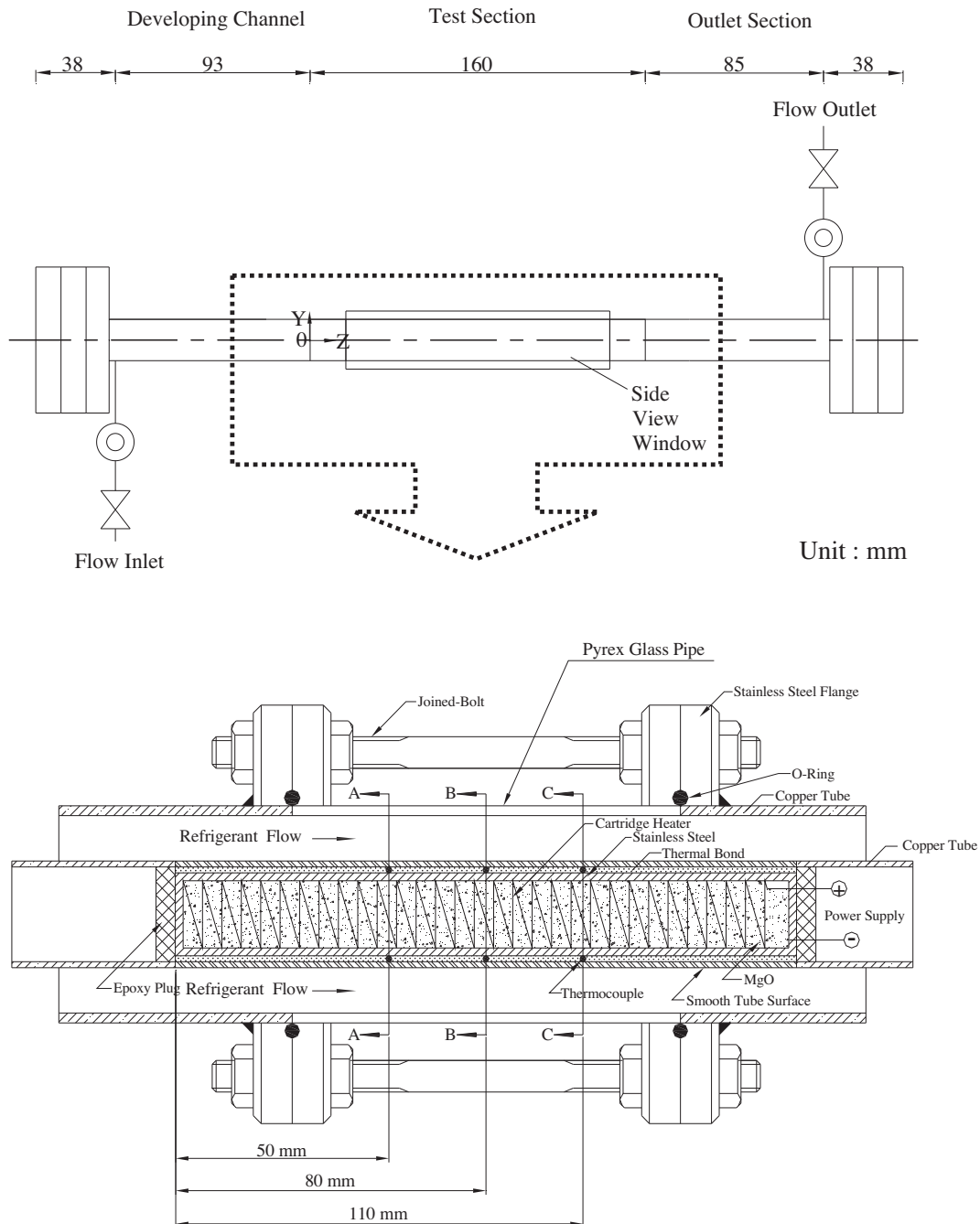


Fig. 2. The detailed arrangement of test section for annular duct.

tude and period of the flow rate oscillation on the time dependent subcooled boiling heat transfer characteristics will be examined in detail. Particularly, visualization of the boiling flow will be conducted to improve our understanding of the time varying flow boiling processes in the narrow channel.

2. Experimental apparatus and procedures

The experimental system used in the previous study [29] for the oscillating saturated flow boiling is also employed here to investigate the subcooled flow boiling of R-134a due to flow rate oscillation in the same narrow annular duct. It is schematically depicted in Fig. 1. The experimental apparatus consists of three main loops, namely, a refrigerant loop, a water-glycol loop, and a hot-water loop. Refrigerant R-134a is circulated in the refrigerant loop. In order to control various test conditions of the refrigerant in the test section, we need to control the temperature and flow rate in the other two loops. The description of the system is detailed in the previous study and is not repeated here.

As schematically shown in Fig. 2, the test section of the apparatus is a horizontal annular duct with the outer pipe made of Pyrex glass to permit the visualization of boiling processes in the refrigerant flow. The glass pipe is 160-mm long with an inside diameter of 20.0 mm. Its wall is 4.0-mm thick. Both ends of the pipe are connected with copper tubes of the same size by means of flanges and are sealed by O-rings. The inner copper pipe has 16.0 mm nominal outside diameter with its wall being 1.5 mm thick and is 0.41-m long. Thus the gap of the annular duct is 2.0 mm ($D_h = 4.0$ mm). Note that the outside surface of the inner pipe is polished by fine sandpaper. In order to insure the gap between the inner and outer

pipes being uniform, we first measure the outside diameter of the inner pipe and the inside diameter of the glass pipe by digital calipers whose resolutions are 0.001 mm with the measurement accuracy of ± 0.01 mm. Then we photo the top and side view pictures of the annular duct and measure the average radial distance between the inside surface of the glass pipe to the outside surface of the inner tube. From the above procedures the duct gap is ascertained and its uncertainty is estimated to be 0.02 mm. An electric cartridge heater of 160 mm in length and 13.0 mm in diameter with a maximum power output of 800 W is inserted into the inner pipe. Furthermore, the pipe has an inactive heating zone of 10-mm long at each end and is insulated with Teflon blocks and thermally nonconducting epoxy to minimize heat loss from it. Thermal contact between the heater and the inner pipe is improved by coating a thin layer of heat-sink compound on the heater surface before installing the heater. Then, 8 T-type calibrated thermocouples are positioned at three axial stations along the inner pipe. The outside surface temperature of the inner pipe T_w is then derived from the measured inside surface temperature by taking the radial heat conduction through the pipe wall into account.

The photographic apparatus established here to record the bubble characteristics in the time periodic flow boiling in the annular duct consists of an IDT X-Stream™ VISION XS-4 high speed CMOS digital camera, a Mitutoyo micro lens set, a 3D positioning mechanism, and a personal computer. The data for some bubble characteristics are collected in a small region around the middle axial location ($z = 80$ mm). After the experimental system reaches a statistical state, we start recording the boiling activity. The digital camera can store the images which are later downloaded to the personal computer. Then, the time variations of the space-average bubble departure diameter d_b and frequency f and active nucle-

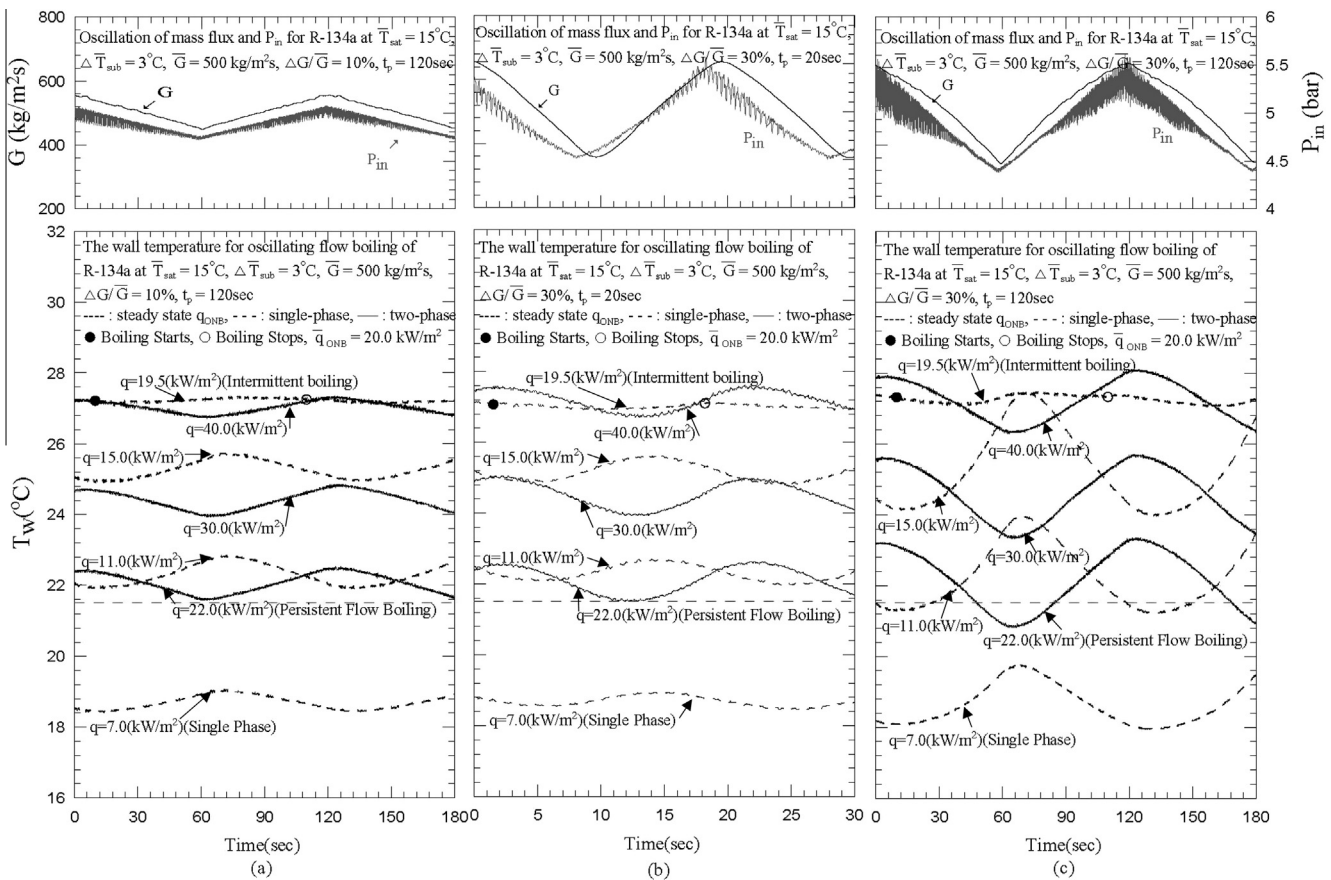


Fig. 3. Timevariations of imposed mass flux, inlet pressure, and wall temperature at $z = 80$ mm for various q , $\Delta G/G$ and t_p at $\Delta T_{sub} = 3^\circ C$.

ation site density n_{ac} in a periodic cycle are calculated by viewing more than 1000 frames at each time instant. Specifically, the images of the bubbles during the boiling processes are directly visualized and measured by showing them on the computer screen in a much slower rate. By considering the pixel depth, size, resolution, center-to-center spacing, sensor image area, minimum inter-frame rate, and integration time of the digital camera and computer screen, the uncertainties of the measured d_p , f and n_{ac} are estimated to be $\pm 10\%$, $\pm 4.5\%$ and $\pm 5.5\%$, respectively.

Before a test is started, the temperature of refrigerant R-134a in the test section is compared with its saturation temperature corresponding to the measured pressure and the allowable difference is kept in the range of 0.2–0.3 K. Otherwise, the system is re-evacuated and then re-charged to remove the air existing in the refrigerant loop. A vacuum pump is used to evacuate noncondensable gases in the loop. Note that in the test the refrigerant at the inlet of the test section is maintained at the required subcooled liquid state by adjusting the water–glycol temperature and flow rate. In addition, we adjust the thermostat temperature in the water loop to stabilize the inlet R-134a temperature. Then, we regulate the time-average refrigerant pressure at the test section inlet by adjusting the opening of the gate valve locating right after the exit of the test section. Meanwhile, by controlling the inverter current of the AC motor connecting to the refrigerant pump, the refrigerant flow rate can be varied to procure the preset mean level and the selected period and amplitude of the mass flux oscillation. The imposed heat flux from the heater to the refrigerant is adjusted by varying the electric current delivered from the programmable DC power supply. By measuring the current delivered to and voltage drop across the heater and by photographing the bubble activity,

we can calculate the heat transfer rate to the refrigerant and obtain the bubble characteristics. All tests are run at statistical state conditions. The whole system is considered to be at a statistical state when the variations of the time-average system pressure and imposed heat flux are respectively within $\pm 1\%$ and $\pm 4\%$, and the variations of the time-average heated wall temperature are less than $\pm 0.2\text{ }^\circ\text{C}$ for a period of 100 min. Then all the data channels are scanned every 0.05 s for a period of 360 s.

3. Data reduction and verification of experimental system

The imposed heat flux q to the refrigerant flow in the narrow annular duct is calculated on the basis of the net power input Q_n and the total outside surface area of the inner pipe of the annular duct A_s as $q = Q_n/A_s$. The total power input Q_t is obtained from the product of the measured voltage drop across the cartridge heater and electric current passing through it. Hence the net power input to the test section is equal to $(Q_t - Q_{loss})$.

The total heat loss from the test section Q_{loss} is evaluated from the correlation for natural convection around a circular cylinder by Churchill and Chu [30]. To reduce the heat loss from the test section, it is covered with a polyethylene insulation layer. The results from the present heat loss test indicate that the total heat loss from the test section is generally less than 1% of Q_t , no matter when single-phase flow or two-phase boiling flow is in the duct. The flow boiling heat transfer coefficient at a given axial location at a given time instant is defined as

$$h_r = \frac{q}{(T_w - \bar{T}_{sat})} \tag{1}$$

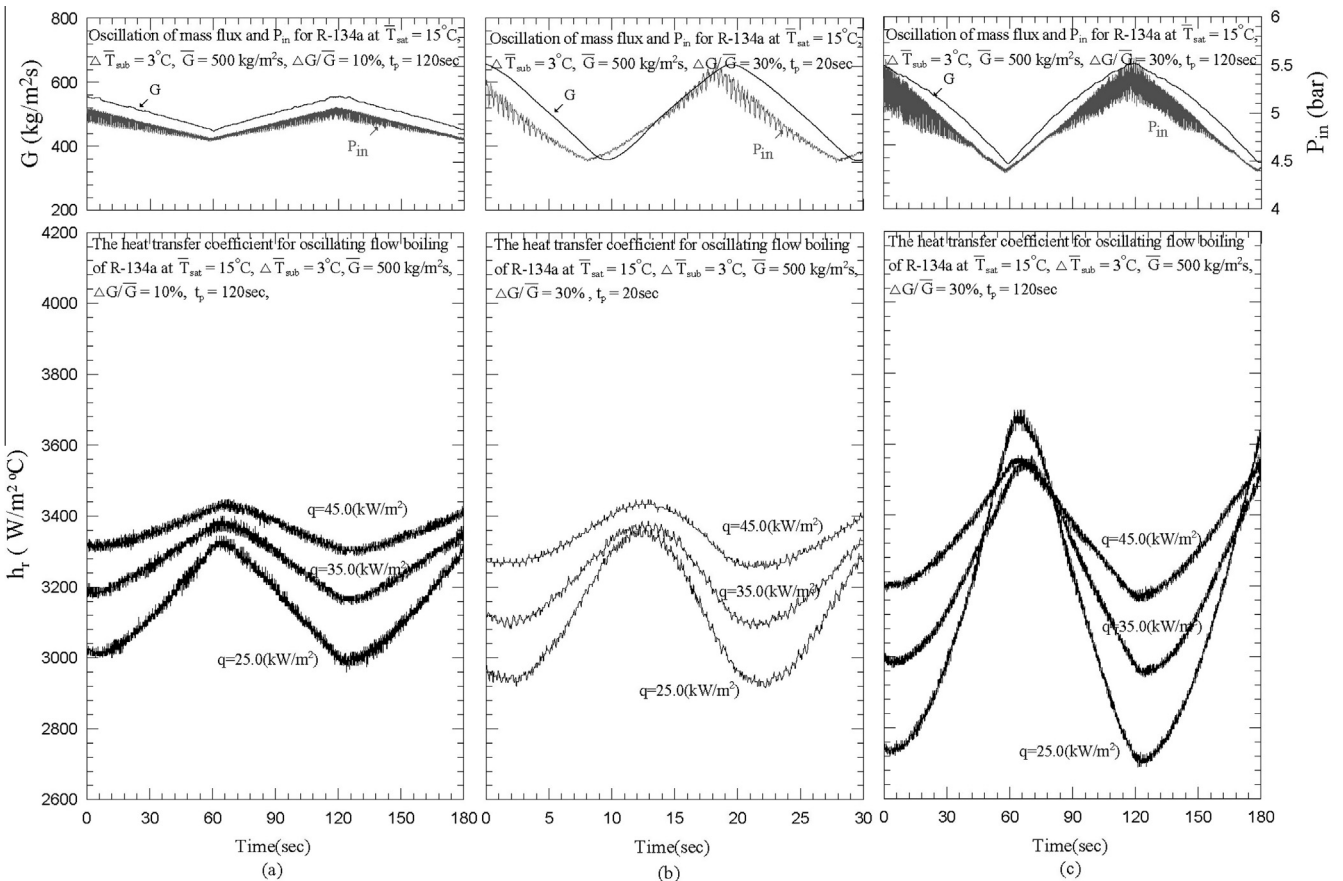


Fig. 4. Time variations of imposed mass flux, inlet pressure, and heat transfer coefficient at $z = 80\text{ mm}$ in persistent boiling for various q , $\Delta G/\bar{G}$ and t_p at $\Delta T_{sub} = 3\text{ }^\circ\text{C}$ at $\delta = 2.0\text{ mm}$.

Uncertainties of the imposed heat flux, measured heat transfer coefficients and other parameters are estimated according to the procedures proposed by Kline and McClintock [31] for the propagation of errors in physical measurement. The results from this estimate show that the uncertainties of the dimension, temperature, pressure, mean mass flux, period of oscillation, amplitude of oscillation, imposed heat flux, and boiling heat transfer coefficient measure-

ments are less than $\pm 1\%$, $\pm 0.2^\circ\text{C}$, $\pm 0.2\text{ kPa}$, $\pm 2\%$, $\pm 0.25\text{ s}$, $\pm 4.8\%$, $\pm 4.5\%$ and $\pm 14.0\%$, respectively.

To check the suitability of the experimental system for measuring the flow boiling heat transfer coefficients, the steady state single-phase liquid R-134a heat transfer coefficients for a constant liquid Reynolds number ranging from 3,648 to 11,420 are measured first and compared with the well-known traditional forced

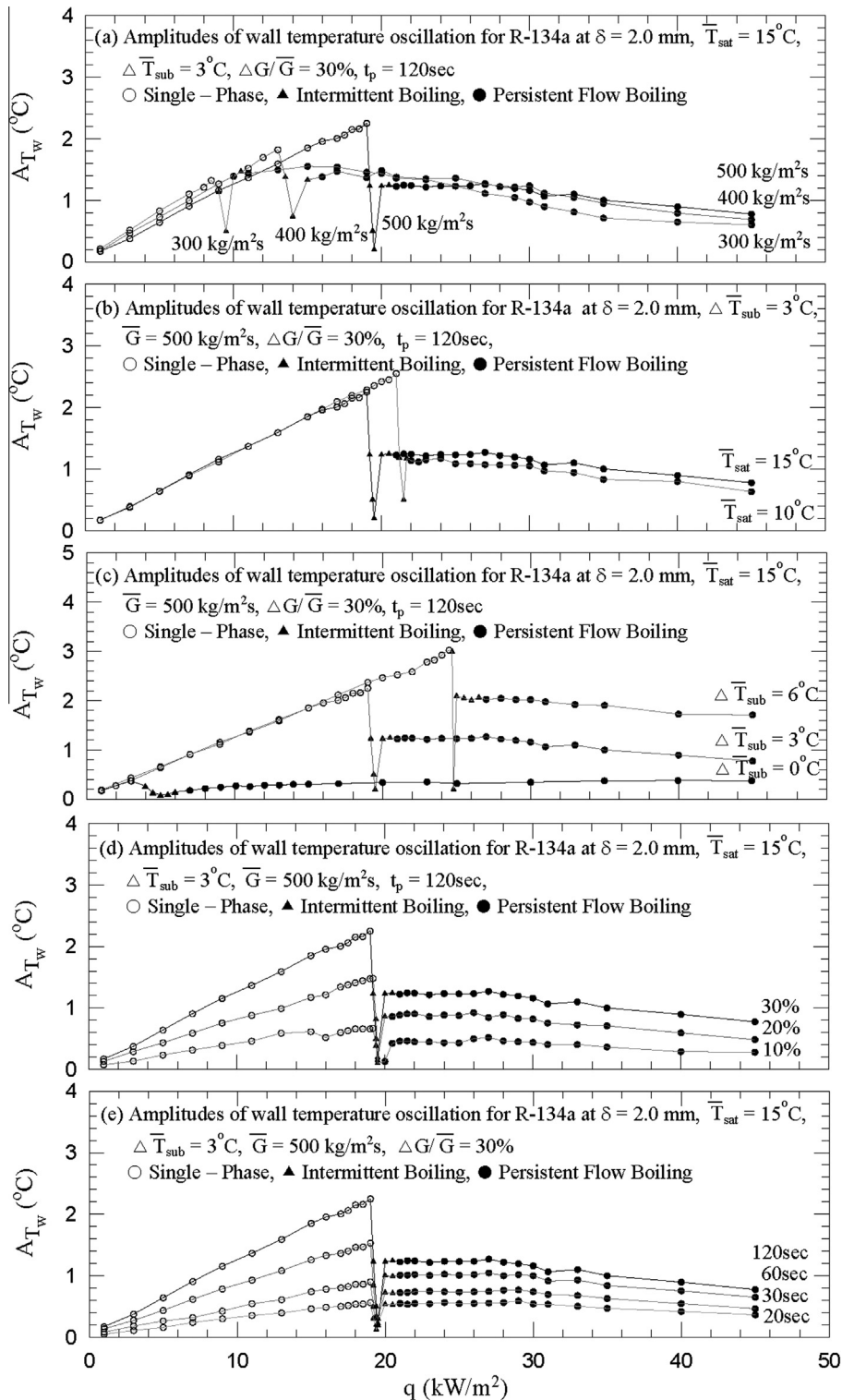


Fig. 5. Variations of amplitudes of heated wall temperature with imposed heat flux for various refrigerant mass fluxes (a), saturated temperatures (b), inlet subcoolings (c), amplitudes of mass flux oscillation (d) and periods of mass flux oscillation (e).

convection correlation proposed by Gnielinski [32]. The results manifest that the present steady heat transfer data can be well correlated by his correlation with a mean absolute error of 3.9%. Because of the lack of the unsteady turbulent forced convection heat transfer data in the open literature, direct validation of the present time periodic liquid heat transfer data is not possible.

4. Results and discussion

In the present experiment the mean refrigerant mass flux \bar{G} varies from 200 to 500 kg/m² s, imposed heat flux q from 0 to 45 kW/m², average inlet liquid subcooling $\Delta\bar{T}_{sub}$ from 0 to 6 °C, and mean system pressure \bar{P} set at 414.6 kPa and 488.6 kPa (corresponding to the mean R-134a saturation temperature $\bar{T}_{sat} = 10$ °C and 15 °C) for the duct gap $\delta = 2.0$ mm. Besides, the amplitude of the refrigerant mass flux oscillation ΔG is set at 0, 10, 20 and 30% of \bar{G} . Moreover, the period of the mass flux oscillation t_p is fixed at 20, 30, 60 and 120 s. The ranges of the parameters chosen above are in accordance with some air-conditioning applications. In the following, attention will be mainly paid to examining the effects of the inlet liquid subcooling on the oscillatory R-134a subcooled flow boiling heat transfer performance. Note that for the limiting case of $\Delta G\bar{G} = 0\%$ we have subcooled flow boiling of R-134a at a constant

refrigerant mass flow rate in the test section, which is designated as stable subcooled flow boiling and has been investigated by Lie and Lin [7]. In the following the thermal characteristics of the oscillatory flow boiling is illustrated by the time variations of the instantaneous heated pipe wall temperature and boiling heat transfer coefficient. Moreover, selected flow photos and data deduced from the images of the boiling processes are presented to show the time dependent bubble characteristics in the boiling flow.

The time constant t_c associated with the response of the heated wall temperature to the imposed time dependent refrigerant flow rate is an important physical quantity in the oscillatory flow boiling. It is measured directly here from the time response of T_w subject to a step change in the mass flux for various q , T_{sat} and ΔT_{sub} . The measured data show that in the transient subcooled boiling flow t_c is longer for lower T_{sat} and higher ΔT_{sub} . Over the ranges of the present experimental parameters t_c varies from 16.3 to 20.3 s. The average t_c is about 18.6 s. The large t_c value mainly results from the inertia of the refrigerant flow rate change with time and the time needed for the heat diffusion and convection from the pipe wall to the refrigerant flow. The time constant associated with the pipe wall of the inner copper pipe alone is rather short, ranging from 0.06 to 0.12 s, due to its high thermal diffusivity. It is of inter-

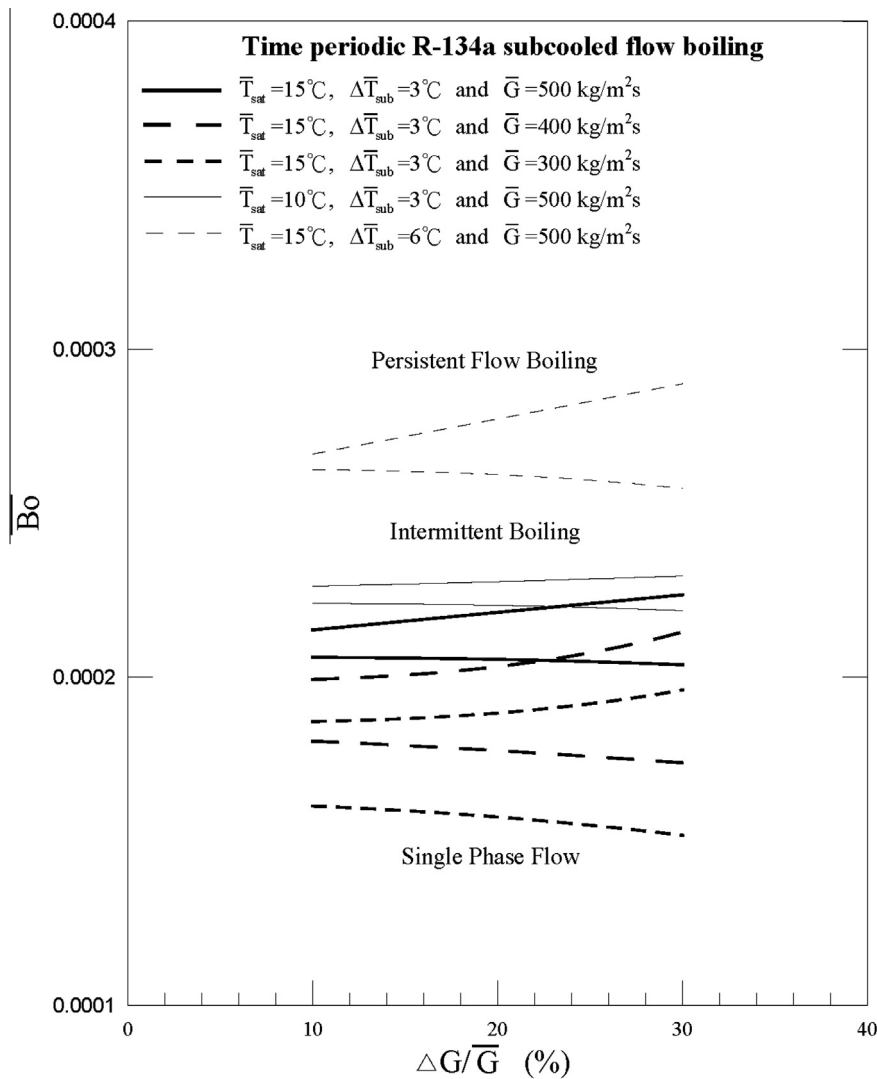


Fig. 6. Flow regime map for time periodic R-134a subcooled flow boiling in annular duct at $\delta = 2.0$ mm.

est to note that when the period of the imposed mass flux oscillation is much shorter than t_c the boiling flow is not able to quickly respond to the fast oscillation and we essentially obtain steady flow boiling heat transfer data for the imposed time-average mass flow rate. On the other end as the period of the mass flux oscillation is substantially longer than t_c the heat transfer in the boiling flow is affected only in the initial stage of the flow rate oscillation. After that quasi-steady flow boiling heat transfer prevails. Thus the transient variations of the boiling heat transfer characteristics are expected to become pronounced when the flow rate oscillation period does not deviate from the time constant of the boiling flow to a large degree. Hence in the present study t_p is chosen to vary from 20 to 120 s, as given previously.

4.1. Time-average subcooled boiling curves and heat transfer coefficient

At first, the time-average boiling curves and heat transfer coefficients measured at the middle axial location ($z = 80$ mm) of the narrow annular duct for various amplitudes and periods of the refrigerant mass flux oscillation were obtained for various $\Delta\bar{T}_{sub}$, \bar{G} , q and \bar{T}_{sat} . The data clearly indicate that in the present time dependent subcooled flow boiling of R-134a the time-average boiling curves and heat transfer coefficients are not affected by the amplitude and period of the refrigerant mass flux oscillation to a significant degree. In fact, they are nearly the same as that for the stable subcooled flow boiling [7].

4.2. Time dependent subcooled flow boiling heat transfer characteristics

The oscillatory subcooled flow boiling heat transfer characteristics for the R-134a flow in the annular duct resulting from the periodic refrigerant mass flux oscillation are illustrated in Figs. 3 and 4 by presenting the measured time variations of the heated wall

temperature T_w and boiling heat transfer coefficient h_r at the middle axial location in the statistical state for various \bar{G} , \bar{T}_{sat} , $\Delta\bar{G}$, t_p , and q at $\Delta\bar{T}_{sub} = 3^\circ\text{C}$. For clear illustration, the measured data for the variations of the imposed refrigerant mass flux are also given here. The mass flux varies like a triangular wave. By and large, the measured oscillatory subcooled flow boiling heat transfer characteristics are qualitatively similar to the oscillatory saturated flow boiling [29]. However, some noted differences do exist. It is of interest to find from these data that in addition to the persistent boiling, intermittent boiling also appears depending on the level of the imposed heat flux, as that for the oscillatory saturated flow boiling with $\Delta\bar{T}_{sub} = 0^\circ\text{C}$. But the temporal oscillations in T_w and h_r are noticeably stronger for the subcooled boiling at $\Delta\bar{T}_{sub} = 3^\circ\text{C}$. Note that the T_w and h_r oscillations are also periodic in time and are at the same frequency as the mass flux. And the T_w and h_r oscillations become more intense for a higher $\Delta\bar{T}_{sub}$ and for a higher amplitude and a longer period of the mass flux oscillation. The stronger T_w oscillation at a larger t_p is attributed to the accumulation and dispersion of thermal energy in the heated pipe wall, respectively in the first half and second half of every periodic cycle over a longer period. However, the amplitude of the T_w oscillation varies nonmonotonically with the imposed heat flux. Note that in the single-phase flow the heated surface temperature oscillates stronger at a higher q at a relatively low imposed heat flux with $q < \bar{q}_{ONB}$. Here \bar{q}_{ONB} is the time-average heat flux for the onset of nucleate boiling for the cases with oscillating mass flux. But an opposite trend is noted in the persistent boiling which prevails at high heat fluxes. The data given in Figs. 3 and 4 also show that the T_w oscillations slightly lag the mass flux oscillation. This time lag apparently results from the large time constant of the flow boiling heat transfer in the duct.

A close inspection of these data further reveals that for the single-phase convection at low q and in the first half of the periodic cycle in which the mass flux decreases with time, the wall temperature is found to rise also with time, suggesting that the single-

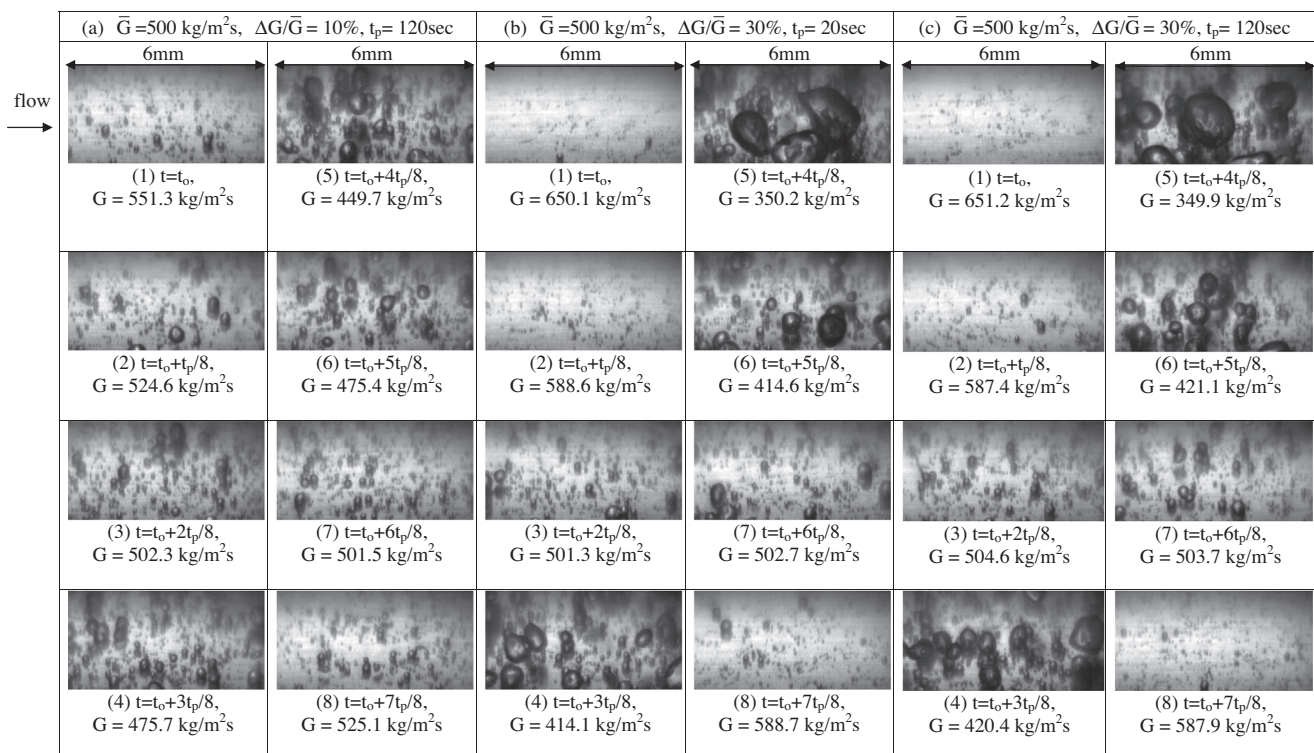


Fig. 7. Photos of bubbles in time periodic subcooled flow boiling of R-134a in a small region around the middle axial location at eight time instants in a typical periodic cycle at $\bar{T}_{sat} = 15^\circ\text{C}$, $\Delta\bar{T}_{sub} = 3^\circ\text{C}$, $q = 25 \text{ kW/m}^2$ and $\bar{G} = 500 \text{ kg/m}^2\text{s}$ for various $\Delta\bar{G}$ and t_p at $\delta = 2.0 \text{ mm}$.

phase convection heat transfer over the heated surface is poorer at a lower G . This trend agrees with the traditional forced convection heat transfer in single-phase flow [32]. The opposite process occurs in the second half of the cycle. The corresponding T_w oscillation amplitude in the single-phase flow can be significant. It is worth noting in the oscillatory subcooled flow boiling that for the imposed heat flux somewhat higher than \bar{q}_{ONB} in the persistent boiling regime, the heated surface temperature can be well below that in the single-phase flow regime prevailed at much lower imposed heat flux in the entire periodic cycle. This outcome obviously results from the relatively significant temperature overshoot at ONB in the oscillatory subcooled flow boiling for R-134a, as seen in the stable flow boiling [7]. We also note that intermittent flow boiling exists less often in the time periodic subcooled flow boiling, when compared with that in the saturated flow boiling [29]. The time instants for the start and termination of the nucleate boiling are marked on the T_w curves for the cases with the presence of the intermittent boiling. At this intermediate imposed heat flux the T_w oscillation is very weak. Note that in the persistent boiling at higher q in the first half of the cycle in which G decreases with time, T_w also decreases with time, suggesting that the flow boiling heat transfer over the heated surface is better at a lower G , as supported by the data for h_r (Fig. 4). The reverse trend is noted in the second half of the periodic cycle in which G decreases with time. This unusual result of increasing (decreasing) h_r at reducing (uprising) G can be attributed to the unique effects of the refrigerant

mass flux variation on the bubble characteristics in the boiling flow, which will be examined later. The results in Fig. 4 also show that the h_r oscillation is significantly weaker at a higher imposed heat flux in the persistent boiling.

The time variations of the refrigerant pressure at the inlet of the test section are also shown in Figs. 3 and 4 for selected cases. The results indicate that the low frequency component of the inlet refrigerant pressure oscillates nearly in phase with the mass flux oscillation and also in the form of triangular waves. In fact, the inlet pressure oscillation is characterized by high frequency components superimposed on the low frequency component. A close examination of these data, however, reveals that the mass flux oscillates slightly behind the low frequency component of the pressure oscillation.

Then, we move further to present the data in Fig. 5 to elucidate the effects of the experimental parameters on the amplitude of the T_w oscillation over a wide range of the imposed heat flux covering the single-phase, intermittent and persistent boiling flow regimes. The results for a given inlet liquid subcooling of 3°C at the high \bar{G} of $500\text{ kg/m}^2\text{ s}$ shown in Fig. 5(a) clearly indicate that in the single-phase flow the oscillation amplitude of T_w increases significantly with the imposed heat flux for given \bar{T}_{sat} , $\Delta\bar{G}$ and t_p . Note that when the intermittent boiling appears the T_w oscillation starts to weaken substantially with an increase in the imposed heat flux. At a certain higher q but still in the intermittent boiling regime the T_w oscillation decays to a minimum point and then a further in-

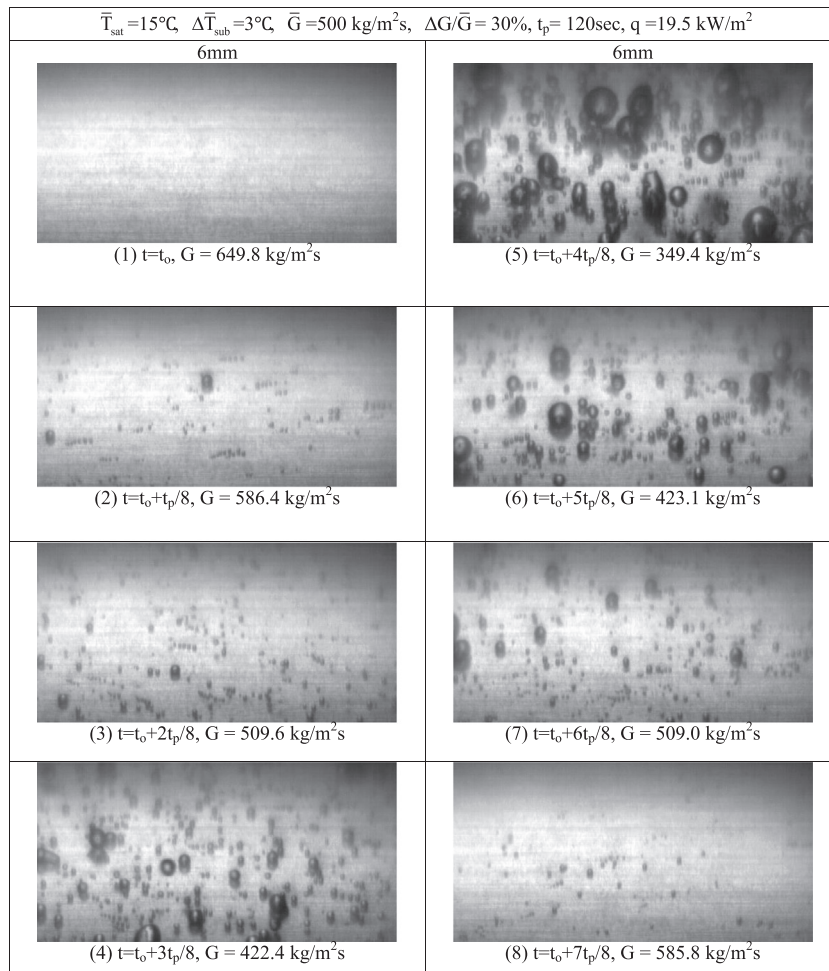


Fig. 8. Photos of bubbles in the time periodic intermittent flow boiling of R-134a in a small region around the middle axial location at eight time instants in a typical time periodic cycle for $\bar{T}_{\text{sat}} = 3^\circ\text{C}$, $\Delta\bar{T}_{\text{sub}} = 3^\circ\text{C}$, $\bar{G} = 500\text{ kg/m}^2\text{ s}$, $q = 19.5\text{ kW/m}^2$, $\Delta\bar{G} = 30\%$ and $t_p = 120\text{ s}$ at $\delta = 2.0\text{ mm}$.

crease in q causes T_w to oscillate in a larger amplitude. This non-monotonic variation of the T_w oscillation amplitude with q in the intermittent boiling can be attributed to the completely opposite trends in the T_w oscillation for the single-phase and persistent boiling flow, as noted in Fig. 3. Specifically, T_w increases as G decreases in the single-phase flow but in the boiling flow T_w decreases at decreasing G . Thus as the bubble nucleation starts to appear in the single-phase flow the T_w oscillation is weakened. This trend continues until the boiling flow dominates over the single-phase flow for a rise in q to a certain level. Then, the T_w oscillation gets stronger for a higher q . In the persistent boiling regime at high imposed heat flux the T_w oscillation gets gradually weaker at increasing q . Note that a much stronger T_w oscillation results for a higher inlet liquid subcooling, as evident from Fig. 5(c). Besides, the T_w oscillation is also somewhat stronger for a higher amplitude and a longer period of the mass flux oscillation (Figs. 5(d) and (e)). However, the mean saturated temperature of the refrigerant shows a relatively insignificant effect on the amplitude of the T_w oscillation (Fig. 5(b)).

4.3. Intermittent flow boiling

In the oscillatory subcooled boiling flow in the heated annular duct for the imposed heat flux close to that needed for ONB of the stable boiling, we also have intermittent boiling, as mentioned earlier. More specifically, in a typical periodic cycle of the refrigerant flow rate oscillation bubble nucleation on the heated pipe wall is first seen at a certain time instant in the first half of the cycle as the imposed refrigerant mass flux decreases to a certain low level and the required incipient boiling heat flux is below the imposed heat flux. The boiling process continues for some time interval. At a certain later time instant in the second half of the cycle in which the imposed refrigerant mass flux increases and the needed incipient boiling heat flux is higher than q , bubble nucleation disappears and boiling stops. Single-phase flow then prevails in the

duct. The above processes of the intermittent flow boiling are repeatedly seen on the heated surface. The data in Fig. 5 clearly manifest that the appearance of the intermittent boiling substantially affects the intensity of the wall temperature oscillation for the subcooled flow boiling. To be more clear, the time instants at which boiling starts and stops are marked on the T_w curves in Fig. 3. It is noted that at a higher imposed heat flux the onset of boiling is earlier and the termination of boiling is later. Besides, the instants for the boiling inception and termination are not affected by the amplitude and period of the mass flux oscillation to a noticeable degree (Fig. 3).

A flow regime map to delineate the boundaries separating different flow boiling regimes in the oscillatory subcooled flow boiling in terms of the mean Boiling number versus the relative amplitude of the mass flux oscillation is given in Fig. 6. The results show that the intermittent boiling prevails at a much higher Boiling number for an increase in the inlet subcooling from 3°C to 6°C. Besides, the intermittent boiling exists over a wider range of the Boiling number for a higher amplitude of the mass flux oscillation, a lower mean refrigerant mass flux and a higher mean refrigerant saturated temperature.

4.4. Bubble characteristics in time periodic subcooled flow boiling

The bubble characteristics associated with the stable subcooled flow boiling of R-134a in the present narrow annular duct have been examined in our recent study [7]. These characteristics indicate that for the imposed heat flux exceeding that for onset of nucleate boiling the duct is dominated by the persistent boiling and a number of discrete bubbles nucleate from the cavities and slide along the heating surface. At a higher q the active bubble nucleation density increases and a lot of coalescence bubbles appear. More coalescence bubbles are seen and they are confined by the duct walls to become slightly deformed for a further increase in q . They also reported that at a higher refrigerant mass flux

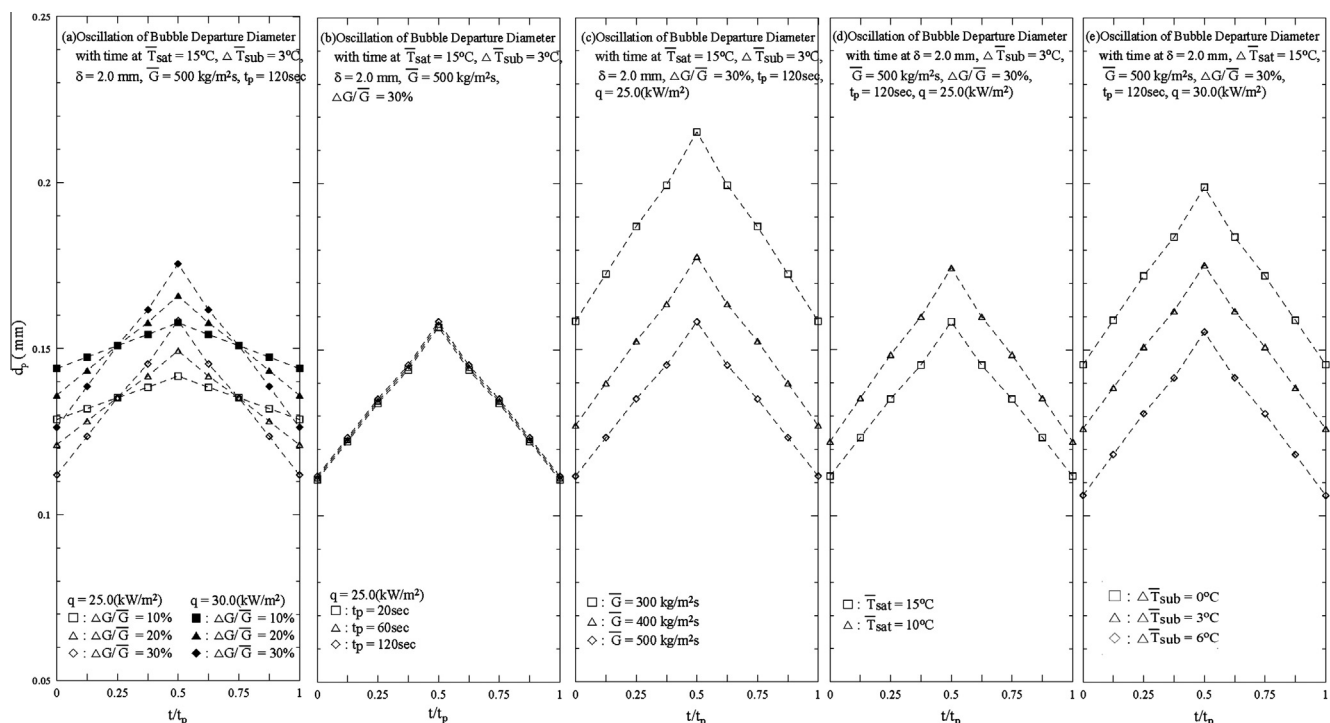


Fig. 9. Mean bubble departure diameter variations with time in a typical periodic cycle for various $\Delta G/\bar{G}$ at $q = 25.0$ and 30.0 kW/m^2 (a), t_p (b), \bar{G} (c), \bar{T}_{sat} (d), and $\Delta \bar{T}_{\text{sub}}$ (e) at $\bar{G} = 500 \text{ kg/m}^2\text{s}$ at $\delta = 2.0 \text{ mm}$.

the bubble departure frequency was higher and the bubbles were smaller and in violent agitating motion. However, the active nucleation site density is lower at a higher mass flux. But at a lower mass flux the bubble coalescence is more important and a number of bigger bubbles form in the duct. Then, at a lower saturation temperature of the refrigerant the bubbles were found to grow bigger and depart at a lower rate, and the active nucleation site density is lower. In general, the bubbles are smaller and less bubble coalescence takes place at a higher inlet liquid subcooling due to the stronger vapor condensation, along with the reduction of the bubble departure frequency and active nucleation sites.

By and large, in the oscillatory subcooled flow boiling investigated here the effects of the imposed heat flux and mean refrigerant mass flux, saturation temperature and inlet liquid subcooling on the bubble behavior exhibit similar trends to that in the stable subcooled flow boiling. Hence, we first illustrate here how the time periodic bubble characteristics are affected by the amplitude and period of the mass flux oscillation for the persistent subcooled flow boiling in Fig. 7 by presenting the photos of the boiling flow for the selected cases for $\Delta\bar{T}_{sub} = 3^\circ\text{C}$ in a small region around the middle axial location at eight selected time instants in a typical periodic cycle in the statistical state. In the figure the symbol “ $t = t_0$ ” signifies the time instant at which the instantaneous refrigerant mass flux is at the highest level and starts to decrease. The results indicate that for given q , \bar{T}_{sat} , $\Delta\bar{T}_{sub}$, \bar{G} , $\Delta\bar{G}/\bar{G}$ and t_p the bubbles get bigger and become more crowded with time in the duct in the first half of the cycle in which the mass flux decreases. The opposite processes take place in the second half of the cycle in which the mass flux increases with time. These changes of the bubble characteristics with the instantaneous mass flux are more significant at increasing amplitude of the mass flux oscillation. Besides, more large bubbles appear in the duct for the cases with a longer period of the mass flux oscillation. Then, the bubble behavior in the intermittent flow boiling for a selected case is shown in Fig. 8. The re-

sults clearly indicate that initially in the beginning of the cycle the instantaneous mass flux decreases with time but is still well above \bar{G} no bubbles nucleate from the heated surface. The flow is in single-phase state. Note that the bubbles start to nucleate from the heated surface at a certain time instant slightly before $t_0 + t_p/8$ at which the instantaneous mass flux is somewhat above \bar{G} . Note that the number and size of the bubbles increase noticeably with time in the second quarter of the periodic cycle for the continuing decrease of the mass flux. Then in the third quarter of the periodic cycle the number and size of the bubbles diminish noticeably with time due to the increase of the mass flux. The bubbles cease to nucleate from the heated surface at a certain time instant slightly after $t_0 + 7t_p/8$ when the mass flux exceeds \bar{G} to a certain degree and bubble nucleation stops completely. Single-phase flow again dominates. We have to wait until the middle of the first quarter of the next cycle to see the bubble nucleation appearing on the heated surface. The above processes repeat in each cycle.

To be more quantitative, we estimate the time variations of the space-average bubble departure diameter and frequency and the number density of the active nucleation sites on the heated surface in a typical periodic cycle at the middle axial location for the persistent subcooled flow boiling from the images of the boiling flow stored in the video tapes. Selected results from this estimation are manifested in Figs. 9–11 by presenting the effects of the experimental parameters on the time dependent bubble characteristics. In these plots the time lag in the flow is ignored. The data in Figs. 9–11 indicate that as the refrigerant mass flux oscillates time periodically, the bubble departure diameter and frequency and active nucleation site density also vary time periodically and to some degree like a triangular wave as the mass flux oscillation. More specifically, the size of the departing bubbles and the active nucleation site density on the heated surface increase but the bubble departure frequency decreases significantly in the first half of the periodic cycle in which the mass flux decreases with time. While in

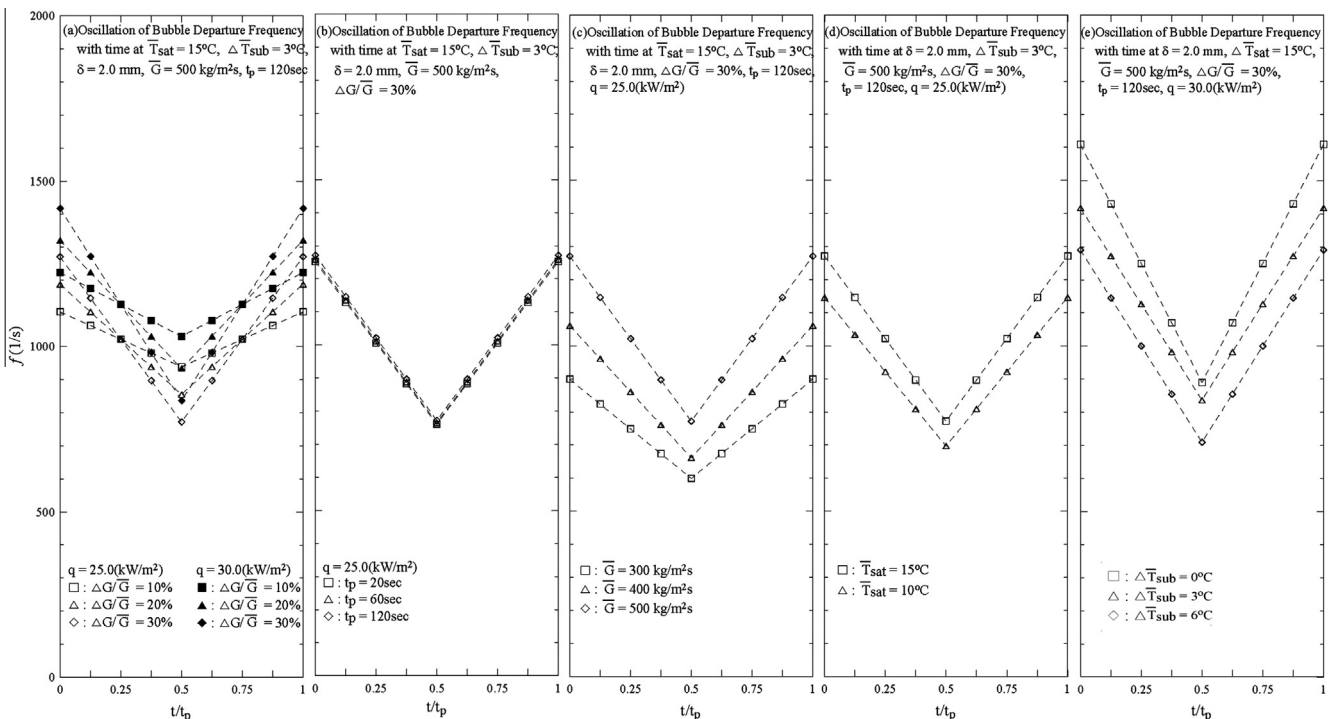


Fig. 10. Mean bubble departure frequency variations with time in a typical periodic cycle for various $\Delta\bar{G}/\bar{G}$ at $q = 25.0$ and 30.0 kW/m^2 (a), t_p (b), \bar{G} (c), \bar{T}_{sat} (d), and $\Delta\bar{T}_{sub}$ (e) at $\bar{G} = 500 \text{ kg/m}^2 \text{ s}$ at $\delta = 2.0 \text{ mm}$.

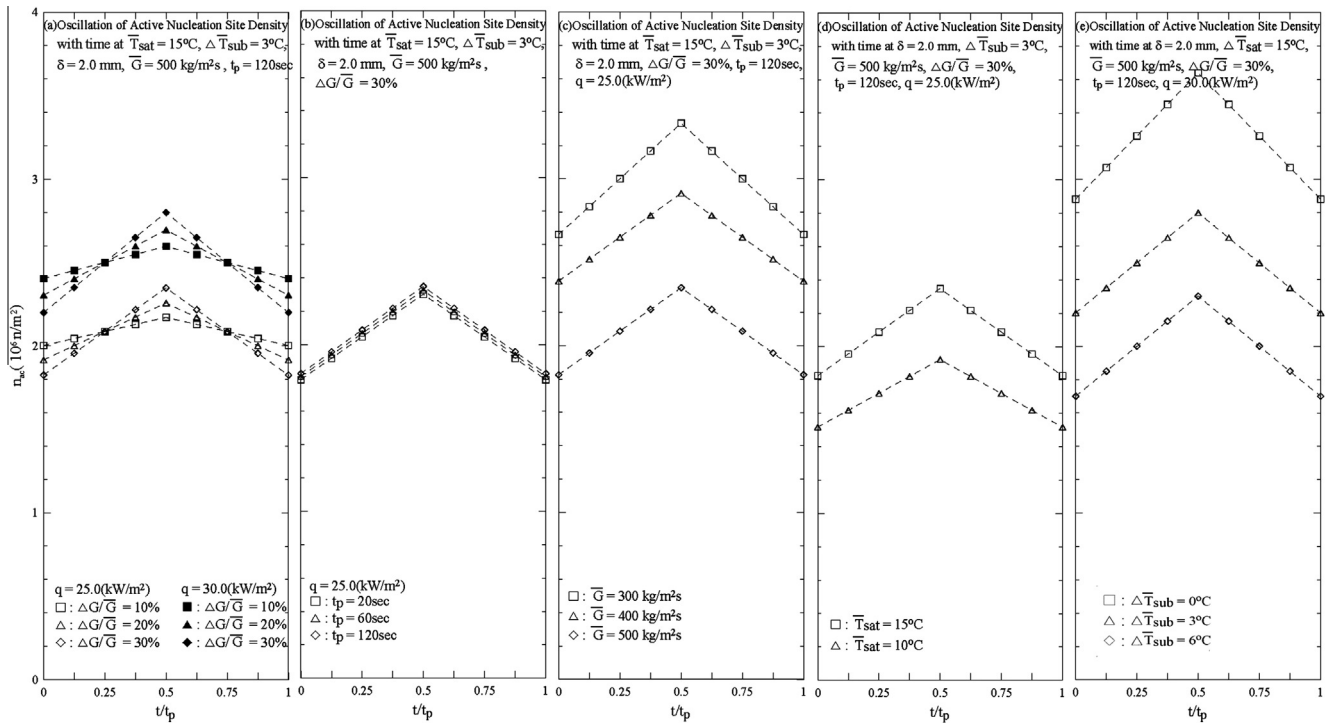


Fig. 11. Mean active nucleation site density variations with time in a typical periodic cycle for various $\Delta G/\bar{G}$ at $q = 25.0$ and 30.0 kW/m^2 (a), t_p (b), \bar{G} (c), \bar{T}_{sat} (d), and $\Delta \bar{T}_{\text{sub}}$ (e) at $\bar{G} = 500 \text{ kg/m}^2 \text{ s}$ at $\delta = 2.0 \text{ mm}$.

the second half of the cycle an opposite process is noted when the mass flux increases with time. Besides, the results in Figs. 9(a), 10(a) and 11(a) show that at a larger amplitude of the mass flux oscillation the bubble departure diameter, frequency and the active nucleation site density oscillate somewhat stronger. Moreover, the results in Figs. 9(b), 10(b) and 11(b) indicate that f , d_p and n_{ac} are not affected by the period of the mass flux oscillation. Furthermore, increases in the mean refrigerant mass flux and saturation temperature and a decrease in the imposed heat flux cause the departing bubbles to become smaller but do not change the wave form of the d_p variation with time (Fig. 9(a), (c) and (d)). At higher q , \bar{G} and \bar{T}_{sat} the bubble departure frequency is higher (Fig. 10(a), (c) and (d)). Note that n_{ac} is significantly larger at a lower \bar{G} and higher q and \bar{T}_{sat} (Fig. 11(a), (c) and (d)). It is also noted that d_p , f and n_{ac} are somewhat smaller for a higher inlet liquid subcooling (Figs. 9(e), 10(e) and 11(e)). It is worth mentioning that in the present study even the size of the largest departing bubble is below 0.25 mm which is much smaller than the diameter of the outer glass pipe in the test section ($D_o = 20.0 \text{ mm}$). Thus the observation of the bubble size through the curved surface of the glass pipe is not expected to produce significant error.

Based on the data presented in Figs. 9–11 for the oscillatory subcooled flow boiling of R-134a in the duct at $\delta = 2.0 \text{ mm}$, the dependence of the quantitative bubble characteristics on the R-134a mass flux oscillation can be approximately expressed as $d_p \propto G^{-a}$, $f \propto G^b$ and $n_{ac} \propto G^{-c}$, when the short time lag in the T_w oscillation is neglected. Here the exponents a , b and c range respectively from 0.5 to 0.54 , 0.79 to 0.84 , and 0.44 to 0.52 . Note that the latent heat transfer resulting from bubble nucleation in the persistent boiling q_b is proportional to d_p^3 , f and n_{ac} , as reported in the literature [7,33]. Thus, $q_b \propto G^{-d}$, here d varies from 1.15 to 1.3 . This result clearly indicates that the flow boiling heat transfer gets better at decreasing refrigerant mass flux since q_b prevails in the boiling heat transfer. This in turn causes the heated wall tempera-

ture to decrease during decreasing refrigerant mass flux and vice versa in the oscillatory subcooled flow boiling, as already seen from Fig. 3 and discussed earlier in Section 4.2. Besides, the dominant effect of the mass flux oscillation on the boiling heat transfer comes from the very strong influences of the mass flux on the bubble departure size.

5. Concluding remarks

The measured heat transfer data for the oscillatory subcooled flow boiling of R-134a resulting from the refrigerant mass flux oscillation in the narrow annular duct have been presented here along with the bubble behavior. Effects of the mean level and oscillation amplitude and period of the refrigerant mass flux on the oscillatory subcooled R-134a flow boiling have been investigated. The major results obtained here can be summarized in the following.

- (1) The time-average boiling curves and heat transfer coefficients for the oscillatory subcooled flow boiling of R-134a are not affected to a noticeable degree by the amplitude and period of the refrigerant mass flux oscillation.
- (2) The heated pipe wall temperature and bubble characteristics also oscillate periodically in time and at the same frequency as the mass flux oscillation. Experiments also show that the resulting oscillation amplitudes of the wall temperature get larger for a longer period and a larger amplitude of the mass flux oscillation and for a higher inlet liquid subcooling. Besides for a larger amplitude of the mass flux oscillation, stronger oscillations in the bubble characteristics, such as d_p , f and n_{ac} , are noted.
- (3) Increases in the bubble departure size and active nucleation site density at decreasing refrigerant mass flux overwhelm the bubble departure frequency in the oscillatory subcooled

flow boiling. This in turn causes an increase in the latent heat transfer and a drop in the heated wall temperature at decreasing G , opposite to that in the single-phase flow.

- (4) The intermittent boiling exists in narrower ranges of the experimental parameters in the subcooled flow boiling. A flow regime map is given to delineate the boundaries separating different boiling flow regimes in the annular duct.

Acknowledgments

The financial support of this study by the engineering division of National Science Council of Taiwan, R.O.C. through the contract NSC 96-2221-E-009-133-MY3 is greatly appreciated.

References

- [1] Z.Y. Bao, D.F. Fletcher, B.S. Haynes, Flow boiling heat transfer of Freon R11 and HCFC123 in narrow passages, *Int. J. Heat Mass Transfer* 43 (2000) 3347–3358.
- [2] T.N. Tran, M.W. Wambsganss, D.M. France, Small circular- and rectangular-channel boiling with two refrigerants, *Int. J. Multiph. Flow* 22 (1996) 485–498.
- [3] B. Agostini, A. Bontemps, Vertical flow boiling of refrigerant R134a in small channels, *Int. J. Heat Fluid Flow* 26 (2005) 296–306.
- [4] S.G. Kandlikar, M.E. Steinke, Flow boiling heat transfer coefficient in minichannels – correlation and trends, *Proceedings of the Twelfth International Heat Transfer Conference 3* (2002) 785–790.
- [5] B. Watel, Review of saturated flow boiling in small passages of compact heat exchangers, *Int. J. Therm. Sci.* 42 (2003) 107–140.
- [6] B.S. Haynes, D.F. Fletcher, Subcooled flow boiling heat transfer in narrow passages, *Int. J. Heat Mass Transfer* 46 (2003) 3673–3682.
- [7] Y.M. Lie, T.F. Lin, Subcooled flow boiling heat transfer and associated bubble characteristics of R-134a in a narrow annular duct, *Int. J. Heat Mass Transfer* 49 (13–14) (2006) 2077–2089.
- [8] T. Otsuji, A. Kurosawa, Critical heat flux of forced convection boiling in an oscillating acceleration field: I – general trends, *Nucl. Eng. Des.* 71 (1982) 15–26.
- [9] Y. Ding, S. Kakac, X.J. Chen, Dynamic instabilities of boiling two-phase flow in a single horizontal channel, *Exp. Thermal Fluid Sci.* 11 (1995) 327–342.
- [10] O. Comakli, S. Karsli, M. Yilmaz, Experimental investigation of two phase flow instabilities in a horizontal in-tube boiling system, *Energy Convers. Manage.* 43 (2002) 249–268.
- [11] P.R. Mawasha, R.J. Gross, Periodic oscillations in a horizontal single boiling channel with thermal wall capacity, *Int. J. Heat Fluid Flow* 22 (2001) 643–649.
- [12] Q. Wang, X.J. Chen, S. Kakac, Y. Ding, Boiling onset oscillation: a new type of dynamic instability in a forced-convection upflow boiling system, *Int. J. Heat Fluid Flow* 17 (1996) 418–423.
- [13] D. Brutin, L. Tadrist, Pressure drop and heat transfer analysis of flow boiling in a minichannel: influence of the inlet condition on two-phase flow stability, *Int. J. Heat Mass Transfer* 47 (2004) 2365–2377.
- [14] J. Shuai, R. Kulenovic, M. Groll, Pressure Drop Oscillations and Flow Patterns for Flow Boiling of Water in Narrow Channel, in: *Proceedings of International Conference on Energy and the Environment*, Shanghai, China, May 22–24, 2003.
- [15] S. Kakac, B. Bon, A review of two-phase flow dynamic instabilities in tube boiling systems, *Int. J. Heat Mass Transfer* 51 (2008) 399–433.
- [16] L. Tadrist, Review on two-phase flow instabilities in narrow spaces, *Int. J. Heat Fluid Flow* 28 (2007) 54–62.
- [17] K. Mishima, H. Nishihara, I. Michiyoshi, Boiling burnout and flow instabilities for water flowing in a round tube under atmospheric pressure, *Int. J. Heat Mass Transfer* 28 (1985) 1115–1129.
- [18] M. Ozawa, H. Umekawa, Y. Yoshioka, A. Tomiyama, Dryout under oscillatory flow condition in vertical and horizontal tubes – experiments at low velocity and pressure conditions, *Int. J. Heat Mass Transfer* 36 (1993) 4076–4078.
- [19] Y.I. Kim, W.P. Baek, S.H. Chang, Critical heat flux under flow oscillation of water at low-pressure, low-flow conditions, *Nucl. Eng. Des.* 193 (1999) 131–143.
- [20] M. Ozawa, H. Umekawa, K. Mishima, T. Hibiki, Y. Saito, CHF in oscillatory flow boiling channels, *Chem. Eng. Res. Des.* 79 (2001) 389–401.
- [21] T. Okawa, T. Goto, J. Minamitani, Y. Yamagoe, Liquid film dryout in a boiling channel under flow oscillation conditions, *Int. J. Heat Mass Transfer* 52 (2009) 3665–3675.
- [22] T. Okawa, T. Goto, Y. Yamagoe, Liquid film behavior in annular two-phase flow under flow oscillation conditions, *Int. J. Heat Mass Transfer* 53 (2010) 962–971.
- [23] M. Ozawa, M. Hirayama, H. Umekawa, Critical heat flux condition induced by flow instabilities in boiling channels, *Chem. Eng. Technol.* 25 (2002) 1197–1201.
- [24] D.W. Zhao, G.H. Su, Z.H. Liang, Y.J. Zhang, W.X. Tian, S.Z. Qiu, Experimental research on transient critical heat flux in vertical tube under oscillatory flow condition, *Int. J. Multiph. Flow* 37 (2011) 1235–1244.
- [25] C.P. Yin, Y.Y. Yan, T.F. Lin, B.C. Yang, Subcooled flow boiling heat transfer of R-134a and bubble characteristics in a horizontal annular duct, *Int. J. Heat Mass Transfer* 43 (2000) 1885–1896.
- [26] R. Situ, Y. Mi, M. Ishii, M. Mori, Photographic study of bubble behaviors in forced convection subcooled boiling, *Int. J. Heat Mass Transfer* 47 (2004) 3659–3667.
- [27] R. Maurus, V. Ilchenko, T. Sattelmayer, Automated high-speed video analysis of the bubble dynamics in subcooled flow boiling, *Int. J. Heat Fluid Flow* 25 (2004) 149–158.
- [28] S.H. Chang, I.C. Bang, W.P. Baek, A photographic study on the near-wall bubble behavior in subcooled flow boiling, *Int. J. Therm. Sci.* 41 (2002) 609–618.
- [29] C.A. Chen, W.R. Chang, T.F. Lin, Time periodic flow boiling heat transfer of R-134a and associated bubble characteristics in a narrow annular duct due to flow rate oscillation, *Int. J. Heat Mass Transfer* 53 (2010) 3593–3606.
- [30] S.W. Churchill, H.H.S. Chu, Correlating equations for laminar and turbulent free convection from a horizontal cylinder, *Int. J. Heat Mass Transfer* 18 (1975) 1049–1053.
- [31] S.J. Kline, F.A. McClintock, Describing uncertainties in single-sample experiments, *ASME Mech. Eng.* 75 (1953) 3–12.
- [32] V. Gnielinski, New equations for heat and mass transfer in turbulent pipe and channel flow, *Int. Chem. Eng.* 16 (1976) 359–368.
- [33] J.R. Thome, *Enhanced Boiling Heat Transfer*, Hemisphere Publishing Corporation, New York, Chapter 6 (1990) 98–117.